Egyptian Geophysical Society
EGS Journal, vol. 6, No. 1, 57-66 (2008)

MAPPING MAGNETIC CONTACTS USING HORIZONTAL GRADIENT MAGNITUDE AND ANALYTIC SIGNAL METHODS IN WADI UM BALAD AREA, NORTH EASTERN DESERT, EGYPT

A.S.M. Assran

Nuclear Materials Authority, P. O. Box 530, Maadi, Cairo, Egypt.

تخريط خطوط التماس بأستخدام طريقتى قيم التدرج الأفقى وتحليل الاشارة المغناطيسية لمنطقة وادى أم بلد بشمال الصحراء الشرقية لمصر

الخلاصة: يوضح تطبيق كل من قيم التدرج الأفقى وتحليل الاشارة المغناطيسية معلومات جيولوجية أكثر من استخدام أى من هاتين الطريقتين بمفردها. وأن أماكن أعلى القيم لكل من هاتين الطريقتين تقع فوق أحرف (خطوط التماس) الأجسام. حيث أن أعلى قيم تحليل الاشارة تقع فوق أحرف الأجسام مباشرة بينما أعلى قيم التدرج الأفقي فتكون ذات ازاحة قليلة ناحية الميل السفلى عندما تكون هذه الأجسام غيررأسية . لذا فان استخدام الطريفتين معاً يحدد خطوط التماس بصورة أكثر دقة.

كما استخدمت أيضا طريقتان لتحديد الأعماق لخطوط التماس و اتجاه الميل السفلى للأجسام المائلة اعتمادا على طريقة (PHILLIPS, 1997). ومن خلال وضع النتائج المتحصل عليها فوق بعضها ومقارنتها أمكن رسم خريطة كناتج نهائى يوضح أماكن خطوط التماس وأعماقها واتجاه الميل السفلى. بالاضافة الى أن هذه الخريطة توضح ثلاثة اتجاهات رئيسية فى المنطقة هى شمال غرب – جنوب شرق، وشمال شرق – جنوب غرب، وشمال شمال غرب – جنوب جنوب شرق مع ثلاثة اتجاهات ضعيفة هى شمال – جنوب و شمال شمال شرق جنوب جنوب غرب وشرق – غرب. وعل الجانب الآخر فإن حساب الأعماق للاجسام المسببة أوضح أن الأعماق من ٤٢م الى ٤٠٠م تقع فوق مكاشف صخور القاعدة بينما الأعماق الكبيرة فتقع فى الأجزاء الوسطى والغربية فوق الصخور الرسوبية..

ABSTRACT: *Application of both the horizontal gradient magnitude (HGM) and analytic signal (AS) methods to the magnetic data yields more geologic information than is obtained, when either method is used individually. The positions of maxima in the HGM and AS are useful for identifying surface locations that lied directly above the edges of source bodies. The AS maxima occur directly over the edges, while the HGM maxima are generally offset down dip from the true locations of the edges of the source bodies, when the structures are not vertical. The two methods can, therefore, be employed together to identify the accurate locations of contacts.*

Aeromagnetic data for Wadi Um Balad area, north Eastern Desert, Egypt, were analyzed using this approach. Two automated interpretation methods, horizontal gradient-depth (HDEP) and analytic signal-depth (ASDEP), as implemented by Phillips (1997), were used for the grids of HGM and AS to determine the magnetic contacts with their strikes and depths, as well as the down dip of the dipping contacts. Overlying the two resulting data sets was done to construct a depth-contact location map, which provides a skeletal outline of what may be interpreted as contacts between units of different magnetizations. This map reveals three major sets of structural lineaments trending mainly in the NW-SE, NE-SW and NNW-SSE directions, beside minor sets trending in the N-S, NNE-SSW and E-W directions. On the other hand, depth estimates showed a range of values that seem plausible with the configuration of the outlined causative sources. It is obvious that, the depth values (42-400m) are concentrated above the tops of the outcropping basement rocks at the eastern part, whereas the deep ones reaching 2.2 km are deviated outwards in the central and western parts of the area above the sedimentary rocks..

INTRODUCTION

Wadi Um Balad area is located at the northern part of the Eastern Desert of Egypt (Fig. 1). It is bounded by latitudes 27° 30' 00" & 27° 54' 44" N and longitudes 32° 15' 00" & 32° 52' 48" E. The area is covered by basement rock units at its eastern part and sedimentary rock units at its central and western parts. The available aeromagnetic data of the study area were surveyed by Aero-Service Division, Western Geophysical Company of America, in 1983. The survey was conducted at a flight altitude of 120m terrain clearance, 1.5 Km flight line interval and 10 Km tie line spacing. These data have been prepared in the grid form for subsequent processing.

The edges of magnetic sources represent abrupt lateral rock-property contrasts that may occur at faults or steeply dipping contacts. Several analytic techniques have been applied to locate the magnetic contacts from gridded

aeromagnetic data. This is done by constructing a function from the aeromagnetic data that is peaked over the contacts. The horizontal gradient method is commonly used to detect magnetic source edges semi-automatically, using the horizontal gradient magnitude (*HGM*) of pseudogravity data (Cordell and Grauch, 1985; and Blakely and Simpson, 1986) or reduced-to-pole (*RTP*) magnetic data (Phillips, 2000; Grauch et al, 2001; Pilkington and Keating, 2004; and Phillips et al., 2007). Another function that peak directly over the magnetic contacts and can be used to estimate their depths, is called analytic signal (Nabighian, 1972; Roest et al., 1992). In each case, the same function, that is used to locate the contacts, can be used to estimate the source depths at the contact locations. Each technique has its own specific limitations, but these can be overcome if the two methods are utilized jointly in magnetic data interpretation.

GEOLOGIC SETTING

Precambrian basement rocks cover the eastern part of the study area and sedimentary rock units of Paleozoic to Quaternary age occupy its central and western parts (Fig. 1). The contact between the basement and sedimentary rock units is running in the NNW-SSE direction. Faults are highly developed in the area, which are divided into five sets: NW-SE, NNW-SSE, NE-SW, N-S and E-W.

The geologic map (Fig. 1) and the description of the study area are based on the geologic map of Gebel El-Urf Quadrangle of Egypt in scale 1: 250,000, which was published by the Egyptian Geological Survey (1983).The Precambrian basement rocks are represented by vast exposures of younger and older granitoid rocks with small exposures of geosynclinal metasediments, metagabbro-diorite complex, Dokhan volcanics and Hammamat group. These rocks are dissected by post granitic dykes and wadis (dry valleys), which are filled with Quaternary wadi deposits. The central part is occupied mainly by NNW-SSE belts of wadi deposits, Galala, Wata and Nubia formations that are arranged from the east to west. Other relatively small exposures of the sedimentary rock units were recorded in this part. Meanwhile, the western part of the study area is occupied mainly by Thebes Formation. A very small exposure of the extrusive basalt and dolerite rocks is observed at the northwestern part of the study area. The exposed rock units with the corresponding ages in the study area are shown in the table .

Table: Litho-stratigraphic sequence of the exposed rocks in the study area

Age		Rock units	Description
Cenozoic	- Quaternary	- Wadi deposits	- Silt and gravel
	- Quaternary	- Fanglomerates	- Gravel, silt and sand
	- Oligocene	- Extrusive rocks	- Basalt and dolerite
	- Eocene	- Thebes Formation	- Limestone with chert
	- Paleocene to Eocene	- Esna Formation	- Shale and marl
Mesozoic	- U-Cretaceous	- Duwi Formation	- Clay with phosphate and sandstone
	- U-Cretaceous	- Nubia Formation	- Clay and sandstone
	- M-Cretaceous	- Wata Formation	- Limestone with clay
	- M-Cretaceous	- Galala Formation	- Dark sandstone with clay
	- L-Cretaceous	- Malha Formation	- Fine sandstone with clay
Paleozoic	- Carboniferous	- Gilf Formation	- Sandstone with sandy clay
	- Silurian	- Naqus Formation	- Sandstone containing pebbles
	- Ordovician	- Araba Formation	- Dark-brown sandstone
Precambrian		- Post granite dykes	- Basic, intermediate and acidic dykes
		- Younger granitoids	- All post-tectonic granites
		- Hammamat group	- Conglomerate, greywacke,siltstone
		- Dokhan volcanic	- Andesite, porphyrite and pyroclastics
		- Older granitoids	- Syn-late tectonic granites
		- Metagabbro-diorite complex	- Gabbroid and dolerite masses
		- Geosynclinal metasediments	- Metagraywake,phylite, schist and slat

DATA PROCESSING TECHNIQUES

1- Horizontal Gradient Magnitude (*HGM*)

The horizontal gradient method is considered as the simplest approach to estimate contact locations and depths, because it only requires calculation of the two-first order horizontal derivates of the magnetic field. If $M(x,y)$ is the magnetic field, then the horizontal gradient magnitude (*HGM*) is given by:

$$HGM\,(x,y) = \sqrt{\left(\frac{\partial M}{\partial x}\right)^2 + \left(\frac{\partial M}{\partial y}\right)^2} \qquad (1)$$

It is peaked over magnetic contacts under the following assumptions: (1) the regional magnetic field is vertical; (2) the source magnetizations are vertical; (3) the contacts are vertical; (4) the contacts are isolated; and (5) the sources are thick (Phillips, 1998). Once the field is reduced-to-pole, the regional magnetic field will be vertical and the source magnetization will be vertical, except for sources with strong remanent magnetization, such as basic volcanic rocks.

2-Analytic Signal (*AS*)

The analytic signal amplitude of the observed magnetic field, defined by Roest et al., (1992):

$$AS\,(x,y) = \sqrt{\left(\frac{\partial M}{\partial x}\right)^2 + \left(\frac{\partial M}{\partial y}\right)^2 + \left(\frac{\partial M}{\partial z}\right)^2} \qquad (2)$$

The analytic signal amplitude peaks over isolated magnetic contacts, as in the horizontal gradient method, the assumption of thick sources lead to minimum depth estimates. Because the analytic signal method requires the computation of the vertical derivative (using Fourier transformations), it is more susceptible to noises than the horizontal gradient method, however, there is no reduction-to-pole transformation required.

In order to infer the information contained in these data in a readable manner, horizontal gradient-depth (*HDEP*) and analytic signal-depth (*ASDEP*) analyses, as implemented by Phillips (1997), have been carried out, where the locations of and depths to layer edges have been determined. In the automated method, crests in the horizontal gradient magnitude and analytic signal amplitude can be located by passing a small 5 by 5 window, and an attempt is made to fit parabolic peaks to the four 5 point scans passing through the center of window. If a sufficient number of peaks is found (usually 2 to 4), the location of the largest peak is taken as the contact location. The techniques have been applied to the grids of the computed horizontal gradient magnitude and analytic signal amplitude. The results of these analyses are point data file. Each record contains a source location and other estimated parameters, such as the strike and depth. It is often useful to convert the point data file into a line file, where the lines follow contacts, faults or other features.

INTERPRETATION

1-Contact Locations

Figures (2) and (3) show the total intensity and *RTP* magnetic data of the study area. The grid of the total magnetic intensity is used to calculate the *AS* amplitude, whereas the *RTP* grid is utilized to calculate the *HGM*. The positions of lithologic or structural contacts of the study area were delineated automatically using the *HDEP* and *ASDEP* computer programs (Phillips, 1997). The results of those programs have been superimposed on the *HGM* and *AS* maps. Discrete source locations estimated by those programs can be connected into lines that follow contacts, faults or other mappable features, based on distance and azimuth criteria. The lines (or connected dots) representing interpreted contacts are shown in Figures (4) and (5).

The horizontal gradient method, because it requires only horizontal derivatives, is relatively insensitive to noise effects in the data. It provides contacts that are highly continuous and generally parallel to the contours of the *RTP* magnetic map (Figs. 3 and 4). The estimated strike directions are closely aligned with the contacts and faults, permitting good definition of the extended linear features, using the strategy of connecting dots. However, the horizontal gradient method requires many assumptions and the violations of these assumptions can result in displacements of the contacts away from their true locations. The displacement is in the down-dip direction for the dipping contact sources (Grauch and Cordell, 1987).

The *AS* results appear to be noisier than the *HGM* results and more focused on the shallow sources. Because this increased noise is the result of added vertical derivative, it does not make the same assumptions and does not result in displaced contacts. Peaks of the *AS* are generally less elongated and more circular than the peaks of the *HGM* (Figs. 4 and 5). Consequently, contacts from the *AS* method are less continuous and the strike directions estimated are less accurate. Accordingly, the two methods were utilized jointly to identify the surface locations occur directly above the source body edges.

Another common signature in the observed *HGM* data exhibits asymmetry, with two peaks of varying amplitudes, an intervening low, and multiple tracks, such as in the southwestern and northeastern parts (marked A,

B, C) of the study area (Fig. 4). This signature is explained by the thin-thick faulted layer model (Grauch et al., 2001), which consists of a thin magnetic layer on the upthrown side of the fault and a thick magnetic layer on its downthrown side.

2- Depth Estimation

Depths to the tops of rock bodies have been estimated from the aeromagnetic data of the concerned area based on the horizontal gradient magnitude and analytic signal methods that operate on the entire grid of the data. The horizontal gradient-depth (*HDEP*) method (Phillips, 1997) uses the *HGM* grid to estimate the strikes of and depths to the source bodies. It relies on the general principle that shallow sources produce anomalies with steep gradients, whereas deep sources produce anomalies with broad gradients. The advantage of this method is its comprehensive coverage of the area and its ability to examine gradients that have various orientations. Its disadvantage is the dependence on the shape of the source body and problems with interference from neighboring sources (Phillips, 2000). The analytic signal-depth (*ASDEP*) method (Phillips, 1997) uses the grid of analytic signal amplitude to estimate the strike directions and depths to the source bodies. The estimated depths of this method are accurate for the contacts and are too shallow for most other sources, as well as dipolar effects are absent (Phillips, 2000).

The depths derived from the *HGM* and *AS* methods are shown in Figures 6 and 7, respectively. The depths estimated from the *HGM* are ranged between 130m and 2273m (Fig. 6), while the depths calculated from the *AS* method varied from 42m to 2146 m (Fig. 7). Both methods of analysis were generally successful in locating the deeper magnetic sources at central, northwestern and southwestern parts, and the shallower magnetic sources in the portions of outcropping basement rocks occurred at the eastern part of the study area (Figs. 1, 6 and 7).

3- Depth-contact location map

The two sets of contact locations resulting from the two analytical methods can be joined to aid in the final interpretation of the preferred contact locations. The following criteria have been used to interpret the final contact locations that are shown in Figure (8): (1) Where the horizontal gradient contacts are isolated, they represent the best available contact locations. (2) Where the horizontal gradient contacts are parallel to and slightly offset from the *AS* contacts, the *AS* contacts represent the true contact locations and the horizontal gradient contacts indicate the down-dip direction. (3) Where the *AS* contacts are isolated and not aligned to flight lines or other known noise directions, they provide reliable contact locations. (4) Where the *AS* contacts are discontinuous due to their noise effects, they may be supplemented by horizontal gradient contacts.

The final contact locations and *AS* depths estimations are both incorporated in Figure (8) to obtain more information about the patterns and general depth ranges of the contacts or faults within the study area. Inspection of this map, in conjunction with the *RTP*, *HGM* and *AS* maps (Figs. 3, 4 and 5), shows the following:-

1) The trends of the geologic contacts or faults reflected three major sets of structural lineaments trending mainly in the NW-SE, NE-SW and NNW-SSE directions, beside minor sets trending in the N-S, NNE-SSW and E-W directions. The NW-SE trend is recorded on the geologic, *RTP*, *HGM* and *AS* maps (Figs. 1, 3, 4 and 5) as a strong trend, therefore it seems to be the most important trend that play an effective role in the structural framework of the study area. Abdel Gawad (1969) considered the NW-SE trend to be one of the most profound fault systems, which affected the Precambrian basement rocks of Egypt. Meshref et al. (1980) mentioned that, this trend is stronger on the Arabian side, as compared to the Nubian side, all along the extension of the Red Sea.

2) The depth estimates, as derived from the *AS* method, show a range of values that seem plausible with the configuration of the outline causative sources. It is obvious that the depth values (42-400m) are reported above the tops of the basement rocks at the eastern part, whereas the deep ones (reaching 2.2 km) are deviated outwards at the central and western parts of the area above the sedimentary rocks. The short wavelength magnetic highs that visible in the *RTP* map (Fig. 3) at the central and western parts (sedimentary rocks), may be due to intra-sedimentary Cenozoic intrusions that are suggested by depth estimations. The geologic map supports this interpretation, where small exposure of extrusive basaltic rock is associated with a magnetic high at the northwestern part of the study area (Fig. 1). Meanwhile, the high depth values that are observed within the basement rocks at the northeastern and southeastern parts are associated with the wadis that dissected the basement rocks (Figs. 1 and 8).

3) The contact lines and depth solutions deduced from both methods are considered as bathymetric data in defining the small basins (B1, B2 and B3) that appeared at the north-central, central and southwestern parts. These basins are bounded by contact lines that have depths reaching 2.2 km (Fig. 8). The *RTP* map supports these solutions, where the longest wavelengths of the area are corresponding to the locations of these basins (Figs. 3 and 8).

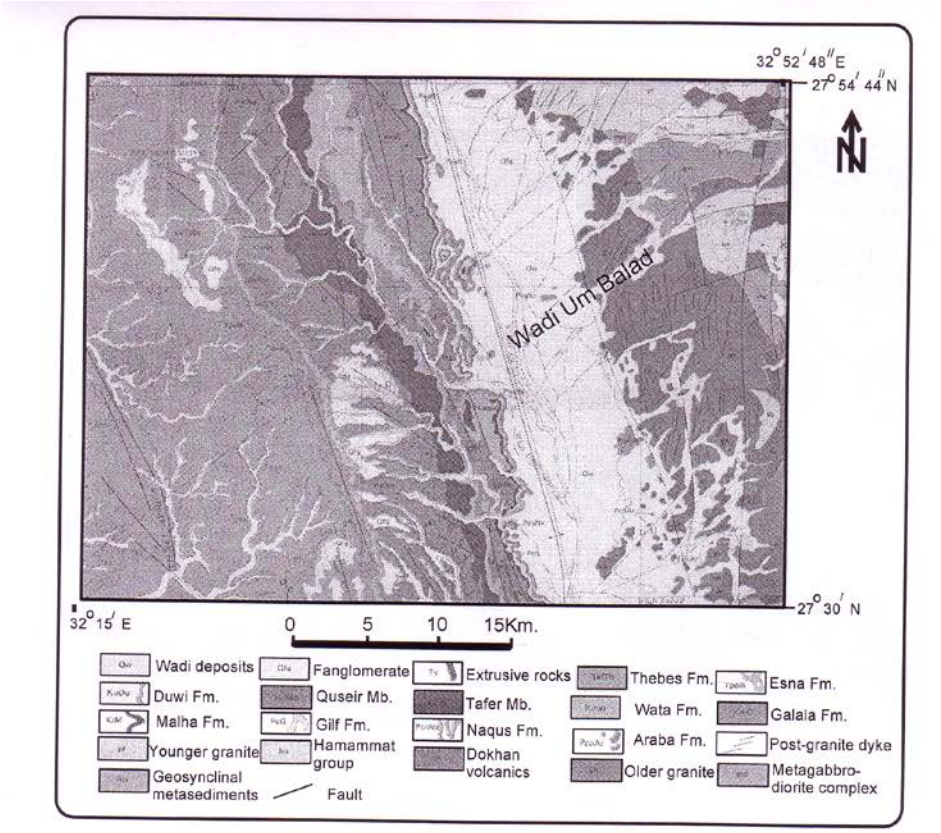

Fig. (1): Geologic map of Wadi Um Balad area, north Eastern Desert, Egypt. (After Egyptian Geological Survey, 1983)

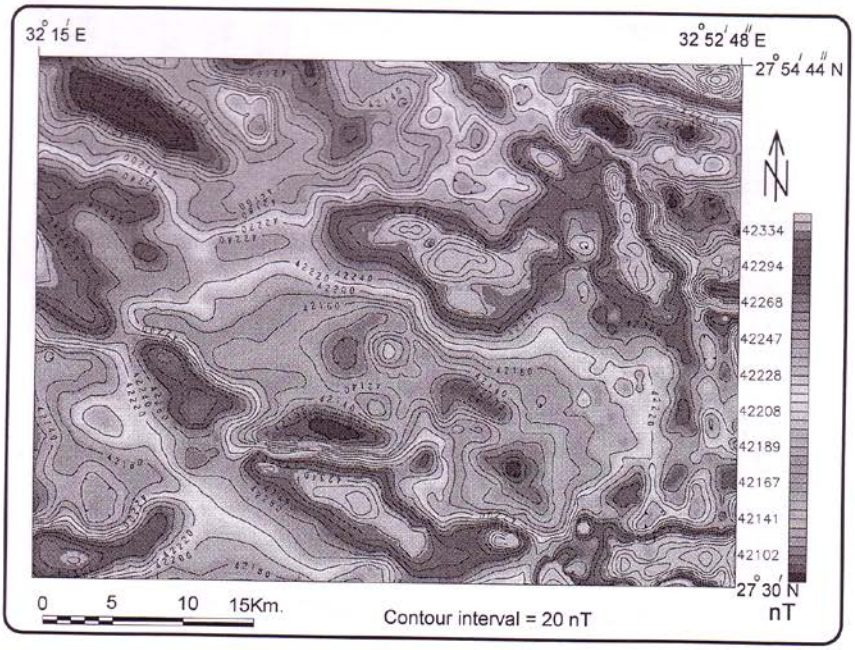

Fig. (2): Total intensity magnetic map of the study area.

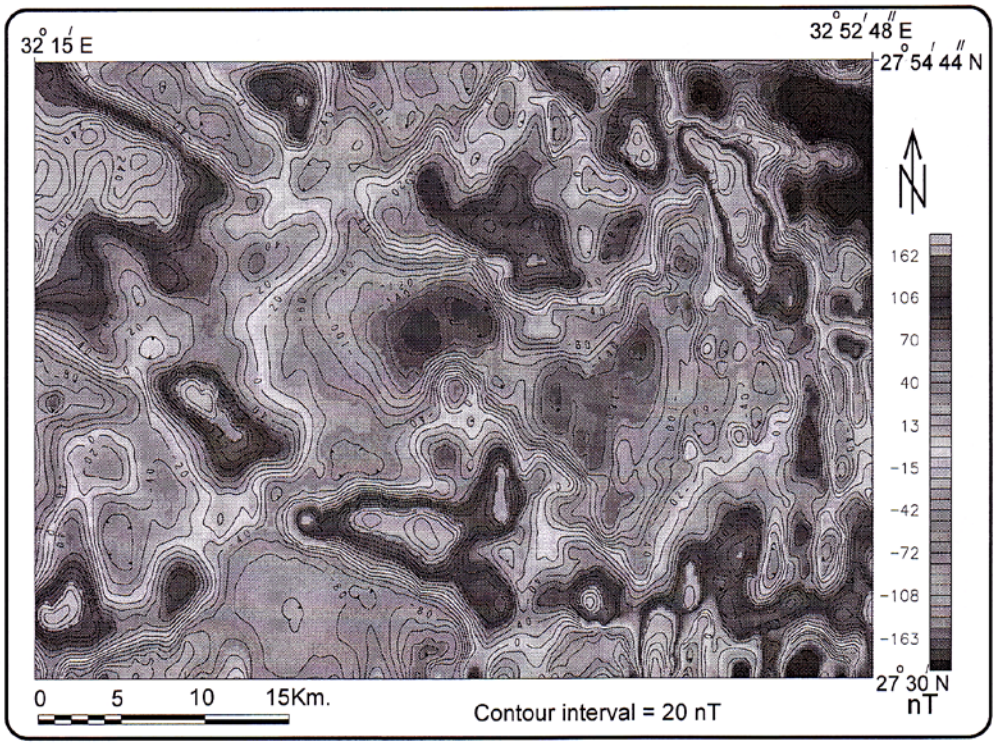

Fig. (3): Reduce to pole (RTP) magnetic map of the study area.

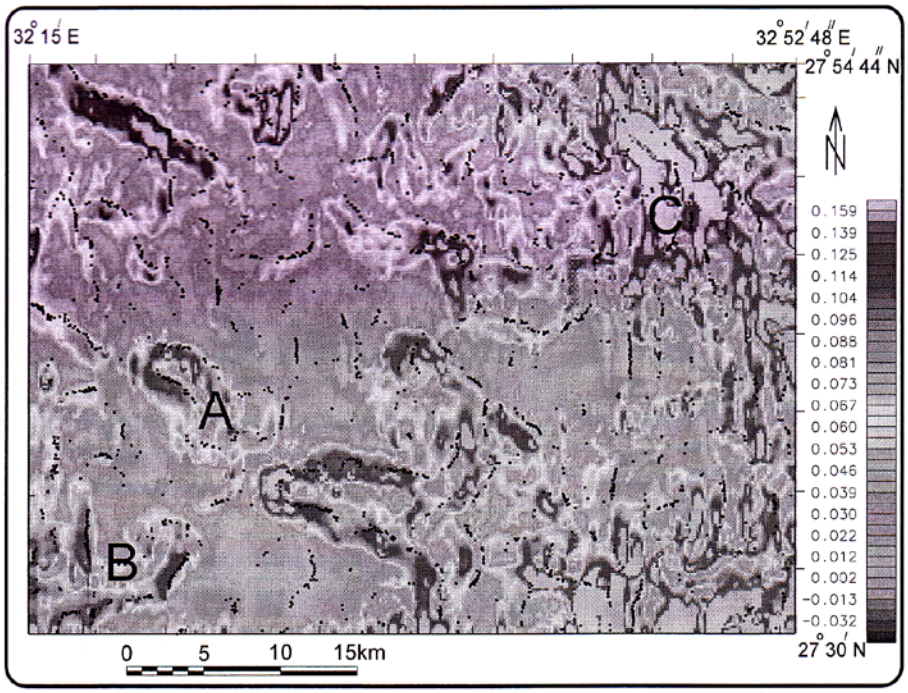

Fig. (4): Horizontal gradient magnitude map of the study area. Black linear dots drawn along the maxima represent magnetic contacts

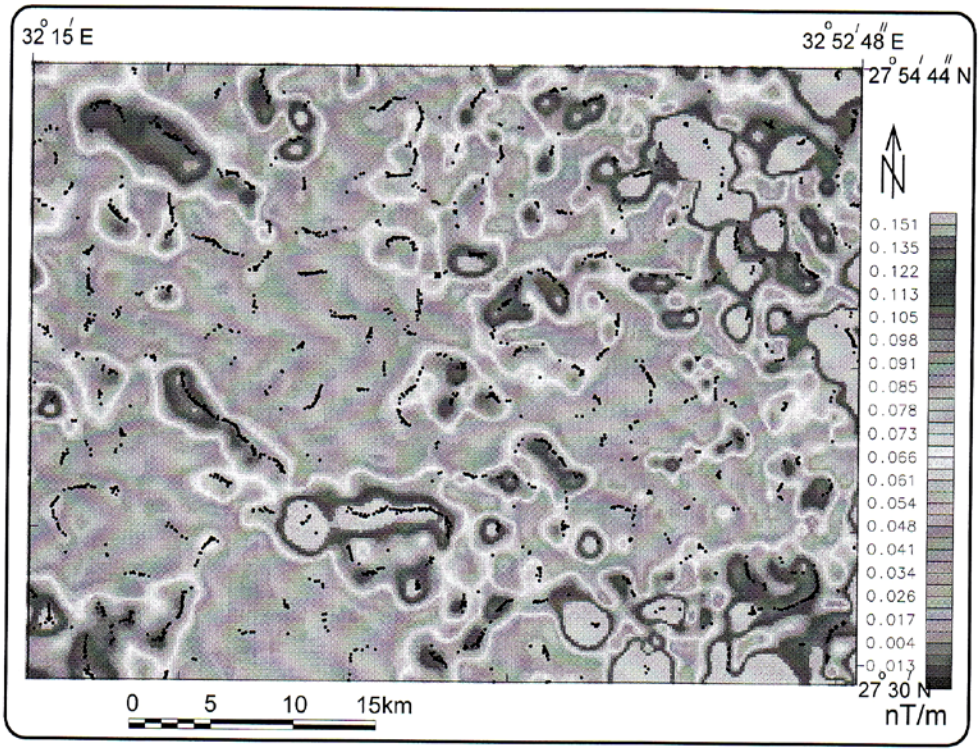

Fig. (5): Analytic signal amplitude map of the study area. Black linear dots drawn along the maxima represent magnetic contacts

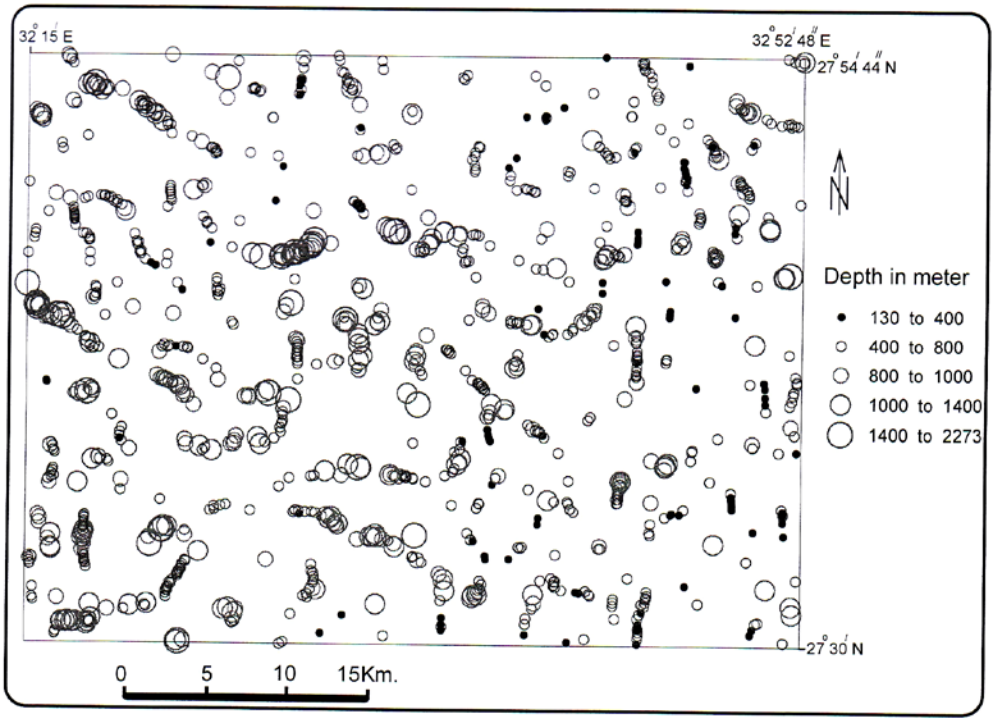

Fig. (6): Depth estimates map as derived from the grid of horizontal gradient magnitude data.

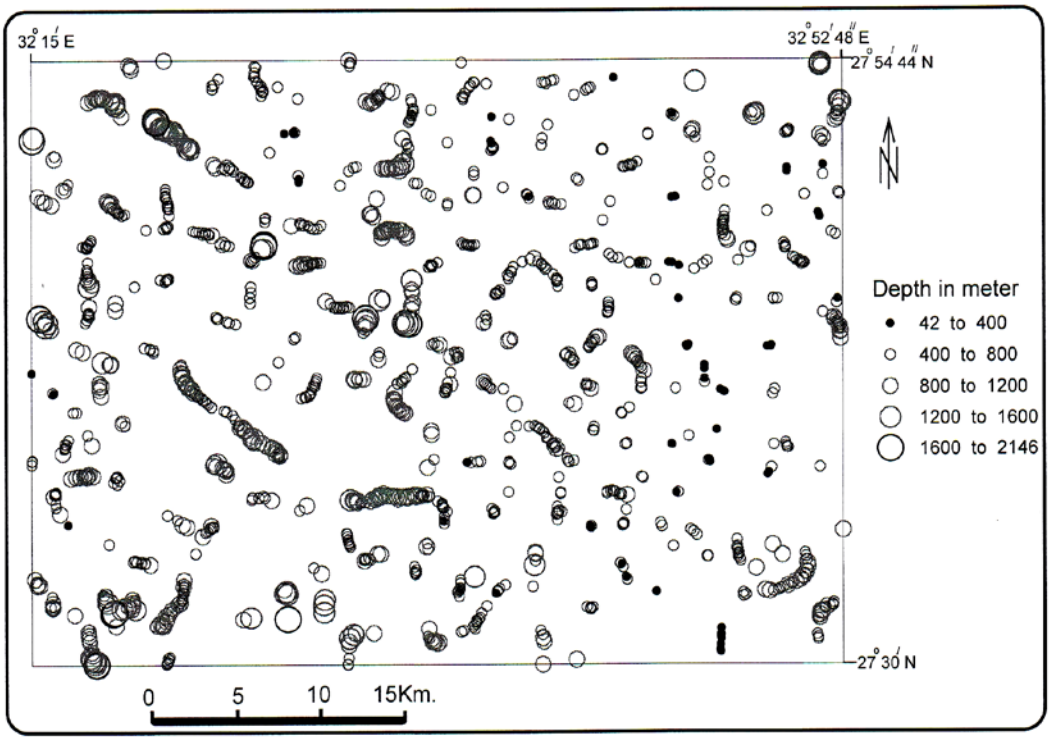

Fig. (7): Depth estimates map as derived from the grid of analytic signal amplitude data.

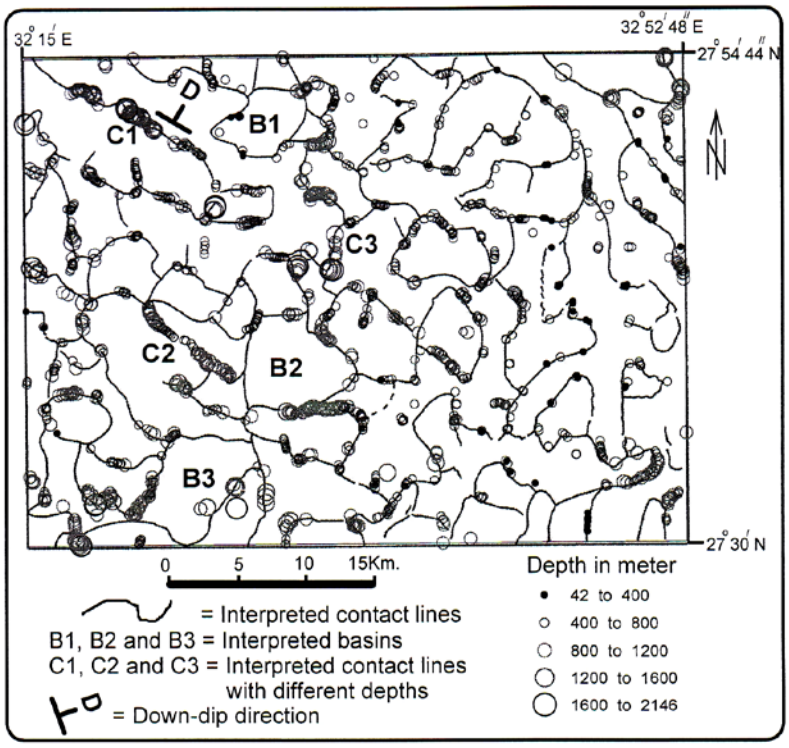

Fig. (8): Depth-contact locations map of the study area showing the depth estimates derived from analytic signal grid and contact lines derived from the horizontal gradient magnitude and analytic signal amplitude data.

4) Different depth solutions are recorded on the same contact line. Thus, these depths can be used to follow the contact line, which may be dissected by faults at deeper level of depths. For example, the contact line located at the northwestern corner of the area (C1), has a shallower depth at its southeastern side and a deeper depth at the northwestern side (Fig. 8). This is supported by the *HGM* and *AS* maps (Figs. 4 and 5), which display different bandwidths for the same contact line. A wider bandwidth indicates deeper source (Roest and Pilkington, 1993). Following the same procedure, other contacts of different depths can be deduced, such as C1, C2 and C3 (Fig. 8).

5) The down-dip can be obtained for a certain class of geologic contacts. For example, at the northwestern corner (marked D), the *HGM* map shows a contact location shifted to the north away from the true position that obtained from the *AS* method (Figs. 4 and 5), suggesting a northward dip for the contact. The offset distance can be obtained simply by measuring the separation between the *HGM* and *AS* maxima. This distance depends on the depth and dip of the geologic interfaces bounded by the source body edges (Grauch and Cordell, 1987).

CONCLUSIONS

Based on the analysis of the horizontal gradient magnitude and analytic signal a depth-contact location map is constructed, which establishes the locations of and depths to layer edges as well as the subsurface geologic and structural picture of the study area. The trends of the geologic contacts or faults reveal three major sets of structural lineaments, trending mainly in the NW-SE, NE-SW and NNW-SSE directions, beside minor sets trending in the N-S, NNE-SSW and E-W directions. On the other hand, depth estimates show a range of values that seem plausible with the configuration of the outline causative sources. It is obvious that, the depth values (42-400m) are concentrated above the tops of the basement rocks at the eastern part, whereas the deeper ones (reaching 2.2 km) are deviated outwards in the central and western parts of the area, above the sedimentary rocks. Different depth solutions are recorded on the same contact line. Thus, these depths can be used to follow the contact line, which may be dissected by faults at deeper level of depths.

Both the horizontal gradient magnitude and analytic signal prove clear contact lines at the central and western parts that are covered by sedimentary rock units, while a less resolution is observed over the outcropping basement rocks due to noise effects that arise from surface and near-surface bodies. Therefore, when applying these methods (especially the analytic signal) to map magnetic contacts over the parts of outcropping basement rocks, it is advisable to remove these noise effects by the upward continuation filter of the aeromagnetic data grid, prior to the calculation of these functions. However, there is no upward continuation filter required over the areas of sedimentary units. Finally, this example shows that, the horizontal gradient magnetic and analytic signal of the aeromagnetic data are useful and complementary tools in the analysis of complex geologic structures. Together, they provide a mean for extrapolating the mapped geologic information at depth, and for inferring the extensions of geologic structures beyond the areas where they can be mapped from outcrops.

ACKNOWLEDGMENTS

I thank Dr. W. Meshref and Prof. Dr. S. Rabie for their review of an early version of this manuscript and for constructive criticisms.

REFERENCES

Abdel Gawad, M., 1969, New evidenceof transcurrent movements in Red Sea area and petroleum implications. Am. Assoc. Petrol. Geol., Bull. 53/7, 1466-1479.

Aero-Service, 1983, Training course in airborne magnetic and radiometric surveying. Presented to the Egyptian General Petroleum Corporation (EGPC),Cairo, Egypt, Aero-Service Division, Western Geophysical Co. of America, Houston, Texas, USA.

Blakely, R.J., and Simpson, R.W., 1986, Approximating edges of source bodies from magnetic and gravity anomalies: Geophysics, 51, 1494-1498.

Cordell, L., and Grauch, V.J.S., 1985, Mapping basement magnetization zones from aeromagnetic data in the San Juan Basin, New Mexico, in Hinze, W. J., Ed., The utility of regional gravity and magnetic anomaly maps: Soc. Expl. Geophys., 181-197.

Egyptian Geological Survey, 1983, Geologic map of the Gebel El Urf Quadrangle, Egypt. In scale 1: 250,000, Geol. Surv. Egypt, Cairo, Egypt.

Grauch, V.J.S., and Cordell, L., 1987, Limitations of determining density or magnetic boundaries from the horizontal gradient of gravity or pseudogravity data: Geophysics, 52, 118-121.

Grauch, V.J.S., Hudson, M.R., and Minor, S, A., 2001, Aeromagnetic expression of faults that offset basin fill, Albuquerque basin, New Mexico: Geophysics, v. 66, p. 707-720.

Meshref, W.M., Abdel Baki, S.H., Abdel Hady, H.M. and Soliman, S.A., 1980, Magnetic trend analysis in northern part of the Arabian-Nubian Shield and its tectonic implications. Ann. Geol. Surv. Egypt. Vol. 10, pp. 939-953.

Nabighian, M.N., 1972, The analytic signal of two-dimensional magnetic bodies with polygonal cross-section: Its properties and use for automated anomaly interpretation; Geophysics, 37, 507-517.

Phillips, J.D., 1997, Potential-field geophysical software for the PC, version 2.2: U.S. Geological survey Open-File Report 97-725,34p.

Phillips, J.D., 1998, Processing and interpretation of aeromagnetic data for the Santa Cruz Basin-Patagonia mountain area, South Central Arizona, Open-File Report 02-98, USGS.

Phillips, J.D., 2000, Locating magnetic contacts: a comparison of the horizontal gradient, analytic signal, and local wavenumber methods: 70th Meting, Society of Exploration Geophysicists, Calgary, Expanded Abstracts.

Phillips, J.D., Hansen, R.O., and Blakely, R.J., 2007, The use of curvature in potential field interpretation. Exploration Geophysics, 38, pp 111-119.

Pilkington, M., and Keating, P., 2004, Contact mapping from gridded magnetic data-a comparison of techniques Exploration Geophysics, 35, 306-311.

Roest, W.R., Verhoef, J., and Pilkington, M., 1992, Magnetic interpretation using the 3-D analytic signal: Geophysics 57, 116-123.

Roest, W.R., and Pilkington, M., 1993, Identifying remnant magnetization effects in magnetic data: Geophysics, 58, pp 653-650.